Scientific Research Publishing

Journal of Environmental Protection, 2023, 14, 841-858
https://www.scirp.org/journal/jep
ISSN Online: 2152-2219
ISSN Print: 2152-2197

Radiological and X-Ray Diffraction Characterization of Bauxite and Rutile Ore Contaminated Environment in Kanam and Wase Mineral Exploration Sites, Plateau State-Nigeria

Adams Udoji Itodo, Raymond Ahulle Wuana, Ishaq Shaibu Eneji, Emmanuel Duwongs Bulus

Department of Chemistry, Joseph Sarwuan Tarka University, Makurdi, Nigeria
Email: emmanuelbulus11@gmail.com

How to cite this paper: Itodo, A.U., Wuana, R.A., Eneji, I.S. and Bulus, E.D. (2023) Radiological and X-Ray Diffraction Characterization of Bauxite and Rutile Ore Contaminated Environment in Kanam and Wase Mineral Exploration Sites, Plateau State-Nigeria. *Journal of Environmental Protection*, **14**, 841-858.
https://doi.org/10.4236/jep.2023.1410047

Received: September 12, 2023
Accepted: October 24, 2023
Published: October 27, 2023

Abstract

Two non-destructive analytical techniques (gamma spectrometer and X-ray diffractometer) were employed in the analysis of bauxite and rutile ore and their vicinity soil and control sourced within the Kanam and Wase mineral exploration sites. The activity concentrations of natural radionuclides ^{238}U, ^{232}Th, and ^{40}K in the soil samples received from bauxite and rutile mineral mining vicinities revealed high concentrations of ^{238}U, ^{232}Th, and ^{40}K compared to the control soil samples sourced 500 m away from the mineral exploration vicinities. Radiological detriments RLI, AUI, Hin and Hex unveiled values exceeding the radiation standard concentration (>1) for soil. X-ray diffraction characterization of bauxite ore revealed the interlocking minerals of Bauxite (18)%, Albite (11)%, Garnet (15)%, Illite (6)% and Muscovite (43)% in various proportions obtained within the 2Θ range (9.18 to 64.4) and a peak value (intensity, cps) of 3400. Pure bauxite percentage in the ore meets metallurgical grade (15 - 25)%. X-ray diffraction of rutile ore revealed the minerals of rutile (40)%, quartz (21.4)%, ilmenite (27)% and garnet (11.8)% found within the 2Θ range (27.5 to 35.6) and a peak value intensity of 31.1 - 100.0 cps also meeting the metallurgical grade of 15% - 25%. The major environmental concern associated with the mineral-sands industry is the radiation hazards, pollution of ground-water sources from heavy metals, mineral transport with heavy equipment's, dredging operations in fragile coastal area and clearing of vegetation.

Keywords

Radiology, Mineralogy, Mining, Bauxite and Rutile Ores, Environmental

Contamination, Radiological detriments, X-Ray Diffractometer, Gamma Spectrometer, Control Soil

1. Introduction

Mining activities are one of the most important pollution sources of metals in countries with a tradition of ore extraction. Millions of tons of wastes deposited on river shores may release toxic elements to the rivers. Once in the water, metals and metalloids may be transported long distances affecting ecosystems [1]. Exploration of solid minerals in Nigeria began during the pre-colonial era (1903/1904) when the British colonial government organize mining operation covering both the northern and southern protectorates. This grew and metamorphosed leading to classification of Nigeria as a leading producer of coal, columbite and tin in 1940s [2]. In plateau state, solid minerals which have been given lesser attention and they also generate a significant level of environmental impact include; bauxite, rutile, gemstone, dimension stone, feldspar, monazite, clay, kaolin, dolomite, mica, zircon, marble, ilmenite, barites, talc, galena, quartz, bismuth ore, gamet, tourmaline, copper, topaz, silica, sharp sand and granite [3].

Soil and sediment are complex matrix that can absorb pollutants and pollution due to heavy or toxic metals has generated much concern in most metropolitan and urban complexes. It is believed that the concentrations of these metals released into the ecosystem may lead to geoaccumulation, bioaccumulation, biomagnification and phytoaccumulation [4]. Plants from industries that even burn their waste on-site are known to be responsible for the release of heavy metals into the atmosphere, which settle in the soil, thus leaving behind lasting effects for years, since they are environmentally stable, non-biodegradable, and tend to cause accumulation in soils [5]. When the surface soils are accumulated, they consequently serve as a transmitter of pollutants to surface water, groundwater, atmosphere, and food. These accumulated pollutants in the surface can as well be transported to different environmental components such as deep soils, plants, and dust particles [6]. Human beings are exposed to radiation arising from sources including cosmic rays, natural radionuclides in water, air, soil and plants; and artificial radioactivity from fallout in nuclear testing and medical applications. The gamma radiation from natural radionuclides and cosmic rays constitute the external exposure while those derived from inhalation and ingestion through foods and drinking water constitutes internal exposure to humans [7].

Natural radioactivity is widely spread in the earth's environment and depends primarily on the geological and geographical conditions, and appears at different levels in the soils of each region in the world [8].

Solid mineral mining and processing constitute a source of pollution to the environment. The mining of tin and other solid mineral ores such as bauxite and rutile facilitates the release of radioactive minerals from the host rocks into the

environment [9]. Studies have indicated rather high level of radioactive waste resulting from mining in Jos and other parts of plateau State-Nigeria. Radionuclides have biological effects on the organs and tissues in the body. Therefore, there is need to determine the specific activities of the radionuclides present in soil [10].

2. Material and Method

2.1. Sample Collection and Site Description

A total of 8 soil samples from Kanam and Wase mineral exploration sites were carefully collected for the gamma spectrometry analysis during the rainy season using stainless-steel core-samplers (push probes and bucket augers) at regular intervals from the surface soils (0 - 15 cm depth) around bauxite and rutile mineral exploration sites. Control soil samples were collected 500 m away from the mining area. The location of the sampling done directly at some points in these areas was based on field survey and determination of location before using Google earth and the Global Positioning System (GPS). This was done to find the location of the distributed samples that have been taken.

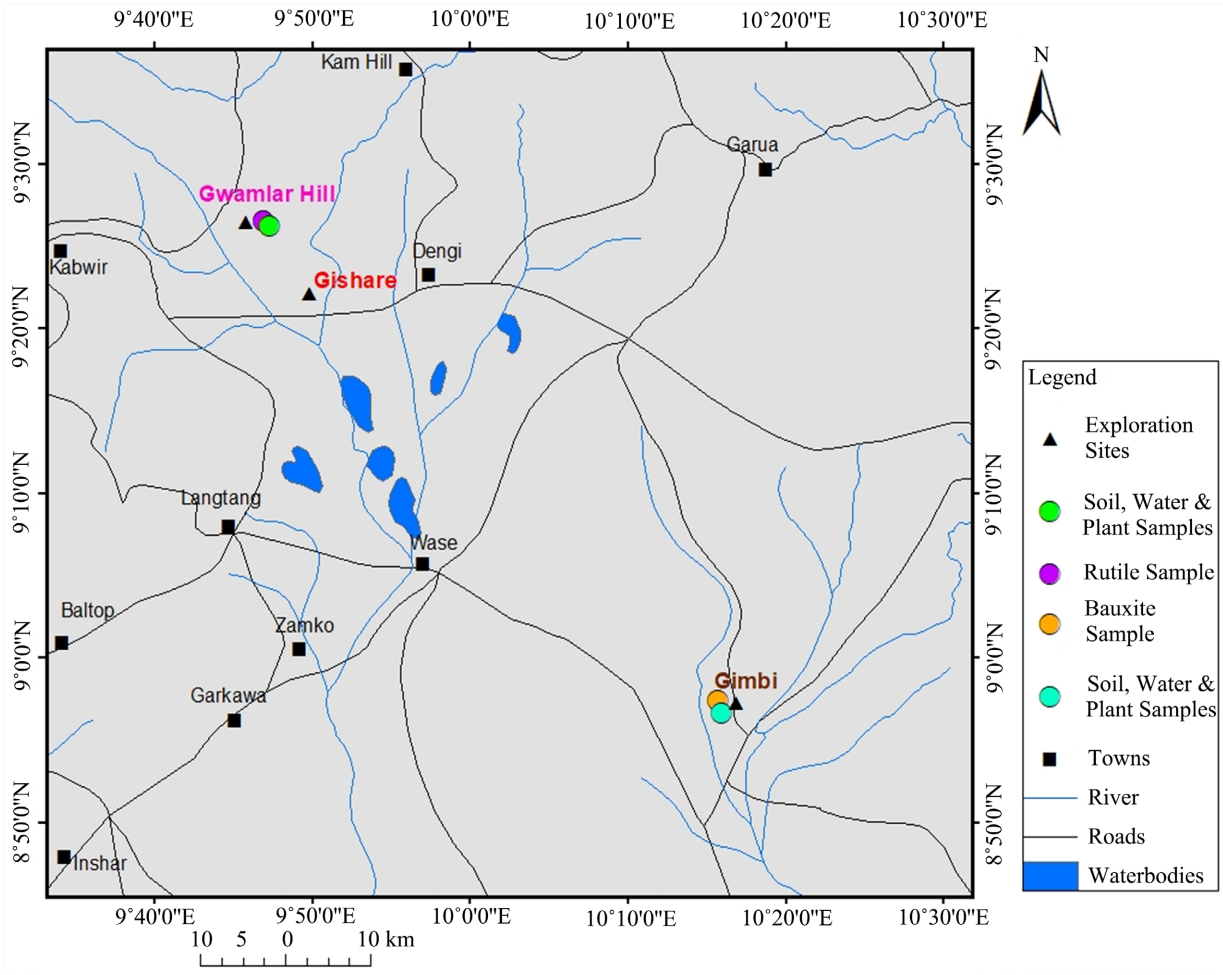

Figure 1. GPS map showing sampling location.

2.2. Sample Preparation and Analysis

Soil samples were air-dried in open air for seven days, to ensure proper drainage and to decrease the moisture content below 20%. This is due to the fact that moisture content above 20% could interfere with the radiological properties and also alter the soil matrix for which the spectrometer has been calibrated with respect to solid (powdered) samples. To achieve this goal, the samples were prepared for drying by breaking them down into aggregates and spreading them evenly on plywood trays in open air, and ensuring with great circumspection that there was no sample cross-contamination or contamination from any external sources.

2.3. Measurement of Soil Radionuclides

The radiological property of the soil samples were prepared and analysed using sodium iodide coaxial type. The radioactivity concentration of radionuclides in the soil samples were measured using a lead-shielded 76 × 76 mm NaI(TI) detector chamber that is coupled to a Canberra Series 10 plus Multichannel Analyzer (MCA) (Model No.1104) through a preamplifier. It has a resolution of about 8% at energy of 0.662 MeV (137Cs) which is considered adequate to distinguish the gamma ray energies of interest in the soil samples. The detector energy and efficiency calibrations were done using standard source ENV 95050 supplied by (IAEA), Vienna. Each source was placed about 7 cm from the detector and counted for 2 h. The energy of the photo peak and the corresponding channel number were recorded and the background count carried out. The soil samples were then counted for 10 h using the calibrated NaI(Tl) detector.

The peak area for each energy in the spectrum was used to compute the activity concentrations in each sample using the following equation:

$$C = \frac{Cn}{Cfk} \quad (1)$$

where, C = activity concentration of the radionuclides in the sample given in Bq/Kg

Cn = Count rate or count per second (cps)

$$Cn = \frac{\text{Net count}}{\text{Live time}}$$

Cfk = Calibration factor of detecting system.

Thereafter the obtained raw data were converted to conventional units using calibration factors to determine the activity concentrations of K-40 (Bq/kg), U-238 (Bq/kg) and Th-232 (Bq/kg) respectively as seen in Tables 1-3 and Figure 2.

3. Discussion

The maximum activity concentration of the three natural radionuclides ^{40}K, ^{238}U, and ^{232}Th found in the soil samples collected from bauxite mineral mining vicinity BS1-3 (924.23 ± 40.52, 87.02 ± 6.01 and 35.95 ± 2.06) had higher gamma ray

Table 1. Activity concentration of ^{40}K, ^{238}U, and ^{232}Th in the soil samples taken from Bauxite and Rutile ore mining vicinities of Kanam and Wase, plateau State-Nigeria.

Sample code		K-40 (Bq/kg)		U-238 (Bq/kg)		Th-232 (Bq/kg)
Bauxite ore vicinity soil	BS1	915.62 ± 45.42	BS1	81.77 ± 8.08	BS1	35.95 ± 2.06
	BS2	903.80 ± 35.02	BS2	81.52 ± 8.06	BS2	35.44 ± 1.90
	BS3	924.23 ± 40.52	BS3	87.02 ± 6.01	BS3	35.63 ± 2.05
Control site bauxite ore	CSBO 98.88 ± 4.99		CSBO 15.55 ± 1.79		CSBO 40.33 ± 2.32	
Rutile ore vicinity soil	RS1	1544.28 ± 74.13	RS1	62.79 ± 4.78	RS1	1.40 ± 0.08
	RS2	1487.32 ± 69.11	RS2	61.78 ± 3.52	RS2	1.41 ± 0.06
	RS3	1526.72 ± 71.19	RS3	62.26 ± 4.16	RS3	1.43 ± 0.09
Control site rutile ore	CSRO 309.52 ± 14.92		CSRO 12.74 ± 1.00		CSRO 39.80 ± 2.22	

NOTE: BS = bauxite vicinity soil, CSBO = control soil from bauxite ore vicinity, RS: rutile vicinity soil and CSRO: control soil from rutile ore vicinity.

Table 2. Minimum, maximum and mean values of ^{40}K, ^{238}U, and ^{232}Th (Bq/Kq) from Rutile vicinity soil.

Code	K-40 (Bq/kg)	U-238 (Bq/kg)	Th-232 (Bq/kg)
Minimum	903.8	81.52	35.44
Maximum	924.23	87.02	35.95
Mean value	914.55	83.43	35.67

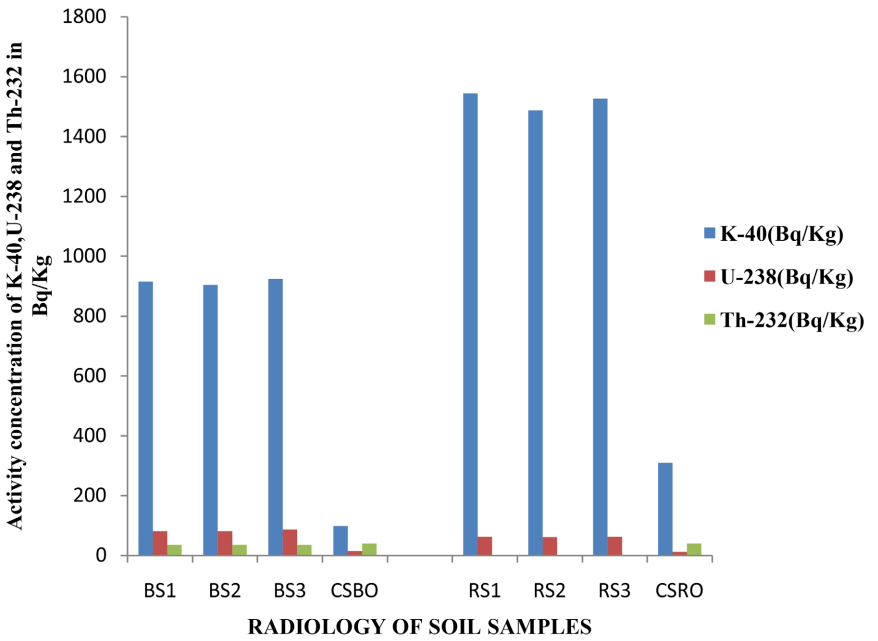

Figure 2. Activity concentration (Bq/kg) of analysed samples from Wase and Kanam mineral exploration sites.

Table 3. Minimum, maximum and mean values of ^{40}K, ^{238}U, and ^{232}Th (Bq/Kq) form Bauxite vicinity soil.

Code	K-40 (Bq/kg)	U-238 (Bq/kg)	Th-232 (Bq/kg)
Minimum	1487.32	61.78	1.40
Maximum	1544.28	62.79	1.43
Mean value	1519.44	62.27	1.41

Table 4. Estimated RLI, AUI, Hin, Hex and Raeq radioactivity from Wase and Kanam mine sites.

Sample code	RLI (Bq/kg)	AUI (Bq/kg)	Hin (Bq/kg)	Hex (Bq/kg)	Raeq (Bq/kg)
BVS	1.522	0.584	0.553	0.553	204.8
CS	0.572	0.639	0.218	0.218	80.83
RVS	1.432	0.719	0.489	0.489	181.2
CS	0.686	0.624	0.252	0.252	93.48

dose (concentration) than the soil obtained 500 m away from mineral ore surrounding referred to as the control sample CSRO (98.88 ± 4.99, 15.55 ± 1.79 and 40.33 ± 2.32). Similarly, the measured activity concentration for the soil samples received from rutile mineral ore vicinity ranged between 1544.28 ± 74.13 (RS1), 62.79 ± 4.78 (RS2) and 1.43 ± 0.09 (RS3), averagely higher than the control soil sample (309.52 ± 14.92, 12.74 ± 1.00, 39.80 ± 2.22). These values presents maximum level of consistency with another research cited in this work (Jos-Nigeria) where the activity concentration of the three natural radionuclides ^{40}K, ^{226}Ra, and ^{232}Th were found within the range of (543.35 ± 0.64 Bq/Kg), (144.20 ± 10.18 Bq/kg) and (1267.91 ± 15.37 Bq/kg) with much lower concentration measured at soil sample GRTS5-7.19 ± 1.23 Bq/kg [11]. Soils and rocks of granite composition contain significant amounts of terrestrial radionuclides. These radionuclides when brought to the surface soil in mine tailings through mineral mining activities may result in enhanced background radiation levels, exposing the miners and the people living around the mines with higher doses of gamma radiation. Exposure to ionizing radiation can cause a variety of health and environmental effects, ranging from skin burns, cancer, genetic mutations and damage to ecosystems, contamination of soil and water, atmospheric pollution and nuclear disasters [12].

3.1. Radiological Detriments/Hazards

The radiological detriments or hazards were estimated to ascertain the levels and degree of soil radiological contaminated due to mineral mining exploration. Hazards such as representative level index (RLI), activity utilization index (AUI), hazard indices (Hin and Hex) and radium equivalent radioactivity (Ra_{eq}) were

computed.

3.2. Representative Level Index (RLI)

The estimated representative level index (RLI) which is the level of gamma radioactivity associated with the different concentrations of ^{40}K, ^{238}U, and^{232}Th (Bq/kg) radioactive elements in the soil samples measured using through the formula;

$$\mathrm{RLI} = \frac{1}{150}\mathrm{Cu} + \frac{1}{100}\mathrm{Cth} + \frac{1}{1500}\mathrm{Ck} \tag{2}$$

The result obtained for the soil samples sourced from the bauxite and rutile mineral mining vicinities revealed values (1.522 and 1.432 respectively) above RLI standard for soil. The control soil samples were however within the maximum RLI limit of 1 [13].

3.3. Activity Utilization Index (AUI)

The dose rates in air from different combinations of ^{238}U, ^{232}Th, and ^{40}K (Bq·kg^{-1}) in the soil samples and control were also computed and by applying the suitable conversion factors, the activity utilization index (AUI) giving by the relation [14].

$$\mathrm{AUI} = \frac{\mathrm{Cu}}{50}\mathrm{fu} + \frac{\mathrm{Cth}}{50}\mathrm{fth} + \frac{\mathrm{Ck}}{500}\mathrm{fk} \tag{3}$$

Revealed values in the range 0.5845 and 0.639 for soil samples received from bauxite mine site vicinity and the control. However, the soil samples sourced from rutile ore vicinity were observed to have apparently higher AUI (0.7199) value than the control soil sample (0.6243) implying that there was enhanced background radiation associated with the rutile mine site vicinity soil compared to the control.

3.4. Hazard Indices (Hin and Hex)

Gamma ray radiation hazards due to these specified radioactive (^{238}U, ^{232}Th, and ^{40}K Bq·kg^{-1}) elements in the soil samples and the control, internal and external hazards were also estimated by calculating the two hazard indices Hin and Hex through the relation;

$$\mathrm{Hin} = \frac{\mathrm{Cu}}{370\ \mathrm{Bq/kg}} + \frac{\mathrm{Cth}}{259\ \mathrm{Bq/kg}} + \frac{\mathrm{Ck}}{4810\ \mathrm{Bq/kg}} \tag{4}$$

$$\mathrm{Hex} = \frac{\mathrm{Cu}}{370\ \mathrm{Bq/kg}} + \frac{\mathrm{Cth}}{259\ \mathrm{Bq/kg}} + \frac{\mathrm{Ck}}{4810\ \mathrm{Bq/kg}} \tag{5}$$

These hazards as obtained/computed from the bauxite ore vicinity soil revealed approximately 1 Bq/kg. These values poses risk of radon exposure and its short lived products which are also dangerous to the respiratory organs [15]. Result received for soil samples collected from rutile ore surface mine site vicinity and the control soil revealed value lower than unity (less than 1 Bq/kg) and

this is recommended by [16].

3.5. Radium Equivalent Radioactivity (Ra_{eq})

The sum of the activity concentrations of ^{238}U, ^{232}Th, and ^{40}K based on the assumption that 10 Bq/kg of ^{238}U, 7 Bq/kg of ^{232}Th, and 130 Bq/kg of ^{40}K produced the same gamma ray dose rates. The radium equivalent radioactivity (Ra_{eq}) of the mineral (bauxite and rutile ores) vicinity soils and control sample were computed from the suggested relation;

$$\text{Raequ}\left(\text{Bq/kg}\right) = \text{CRa} + 1.43\text{CTh} + 0.077\text{CK}. \quad (6)$$

The results obtained reflects the non-detrimental range since the highest value of Ra_{eq} were observed to be <370 Bq/kg thereby keeping the external dose at <1.5 mGy/h [17].

3.6. X-Ray Diffraction (XRD) Analysis of Bauxite and Rutile Mineral Ores

Bauxite and Rutile ore samples were collected directly from the mineral exploration vicinities of Kanam and Wase LGAs. The ore samples were identified and finely grind to pass through a 200 - 250 mesh sieve at Bass and Matt mineral Ltd Yingi-Rayfield, Jos Plateau State. The representative samples were subjected to X-ray scanning using X-ray diffractogram model Rigaku miniflex 650 by Rigaku cooperation Japan with a cu-anode and the mineral phases within the samples were identified through powdered X-ray diffractometry method after which the mineral peaks were identified using the desired software. The background and peak-positions were identified based on the peak positions and intensities. This procedure was carried out successively and repeated for each of the mineral representative sample.

4. Results and Discussion

The results for the X-Ray Diffraction of bauxite and rutile ore minerals sourced from the Wase and Kanam mining areas are presented in **Tables 5-8**, and **Figures 3-9**.

5. Discussion

5.1. XRD Peak Information of Bauxite Ore

The XRD result for bauxite ore collected within the mining vicinity of Wase local government area as observed from the in **Figure 5** revealed the interlocking minerals of Bauxite (18)%, Albite (11)%, Garnet (15)%, Illite (6)% and Muscovite 2M1 (2)%. The X-ray diffractogram showed that the ore and other minerals were found within the 2Θ range (9.18 to 64.4) and a peak value (intensity, cps) of about 3400. Diffraction of X-rays by the crystalline solid mineral sample results in a pattern of sharp bragg reflection characteristic of the different d-spacing of the ore. Broadening of these reflections due to instrumental factors is generally

Table 5. XRD Peak information of Bauxite ore.

S/N	Pos. [˚2Th.]	Height [cts]	FWHM Left [˚2Th.]	D-Spacing [Å]	Rel. Int. [%]
1	9.1889	105.7	0.1968	9.62437	63.94
2	18.1077	68.59	0.1968	4.89911	41.47
3	20.1438	19.24	0.3149	4.40829	11.63
4	24.4678	26.26	0.3936	3.63816	15.88
5	25.6613	12.08	0.4723	3.47159	7.300
6	27.0537	165.4	0.3149	3.29600	100.0
7	28.3219	59.02	0.1574	3.15123	35.68
8	35.3470	25.75	0.2362	2.53938	15.57
9	36.9175	80.26	0.1378	2.43488	48.53
10	42.8334	24.35	0.2362	2.11130	14.72
11	45.7373	71.26	0.2755	1.98378	43.09
12	50.4870	45.44	0.1181	1.80773	27.47
13	55.6535	10.13	0.9446	1.65154	6.120
14	60.3084	16.82	0.4723	1.53473	10.17
15	62.2121	15.80	0.5510	1.49226	9.550
16	64.3544	45.93	0.1181	1.44766	27.77

Table 6. Peak information of Rutile ore.

S/N	Pos. [˚2Th.]	Height [cts]	FWHM Left [˚2Th.]	D-Spacing [Å]	Rel. Int. [%]
1	27.5711	63.68	0.2362	3.23531	100.00
2	32.6596	45.26	0.2362	2.74193	71.08
3	35.6894	19.83	0.9446	2.51580	31.13

Table 7. Minerals associated with ore samples.

Ore Sample	Associated Mineral	Chemical Formular	Mineral Percentage
Bauxite	Albite	$NaAlSi_3O_8$	10.6(11%)
	Garnet	$X_3Y_2Si_3O_{12}$	0.67(15%)
	Illite	$K,H_3O(Al,Mg,Fe)_2(Si,Al)_4O_{10}((OH)_2{\cdot}(H_2O))$	4.7(6%)
		Muscovite $KAl_2(Si_3Al)O_{10}(OH)_2$	43(2%)
Rutile	Quartz	SiO_2	21.4(13%)
	Ilmenite	$(Fe,Ti)_2O_3$	27(3%)
	Garnet	$X_3Y_2Si_3O_{12}$	11.8(7%)

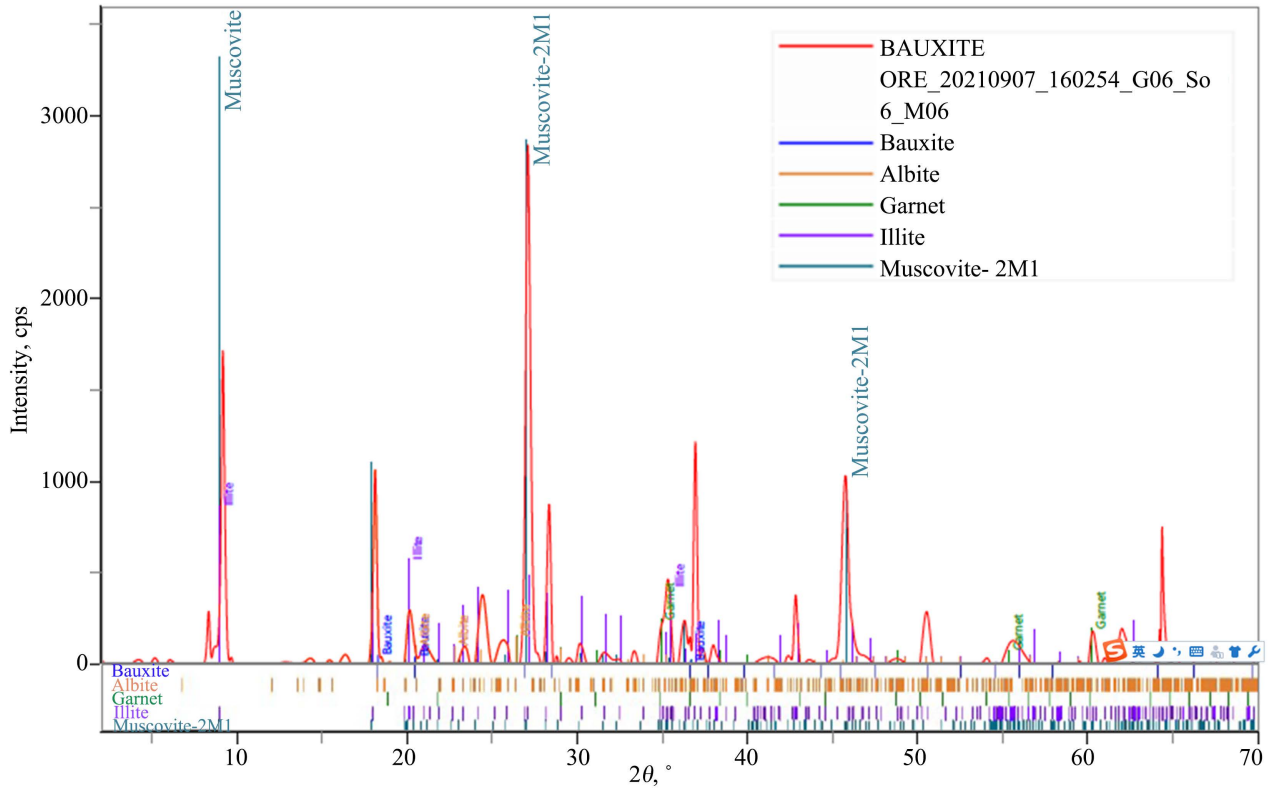

Figure 3. X-ray diffractogram of Bauxite sample.

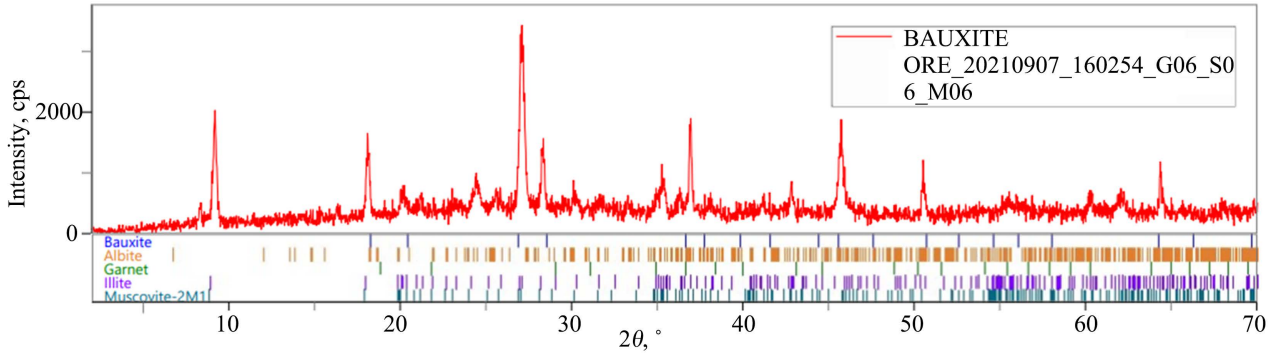

Figure 4. X-ray diffractogram of Bauxite ore.

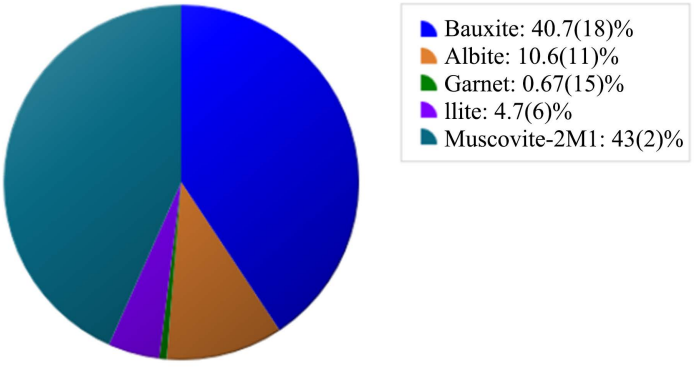

Figure 5. Pie chart showing the associated minerals in bauxite ores.

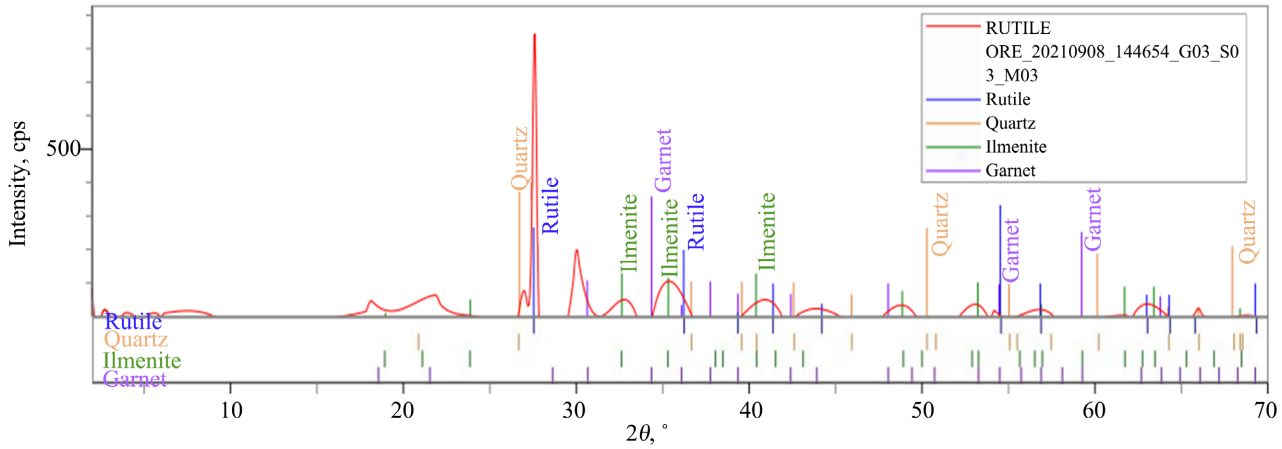

Figure 6. X-Ray diffractogam of Rutile sample.

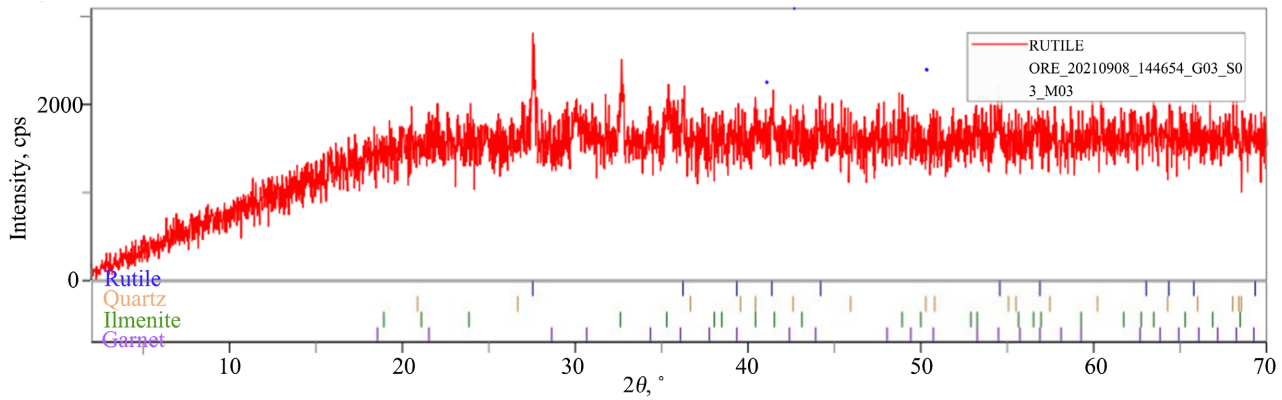

Figure 7. X-ray diffractogam of Rutile ore.

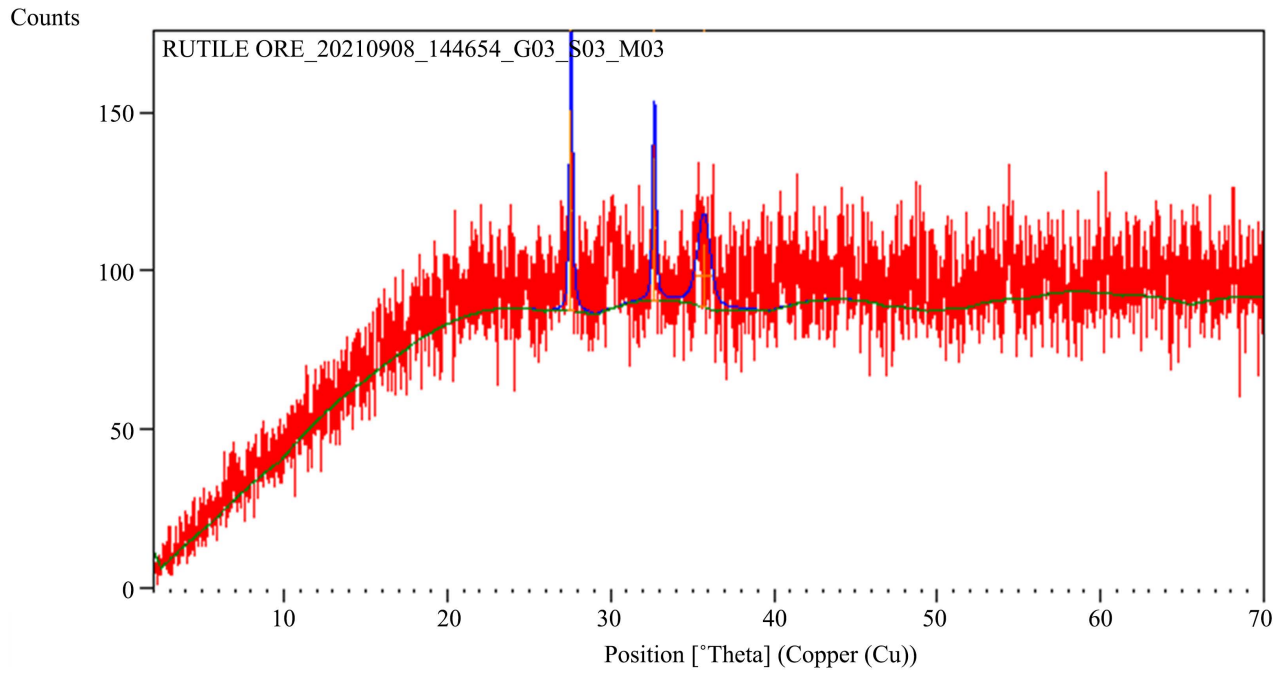

Figure 8. Rutile main graphic view.

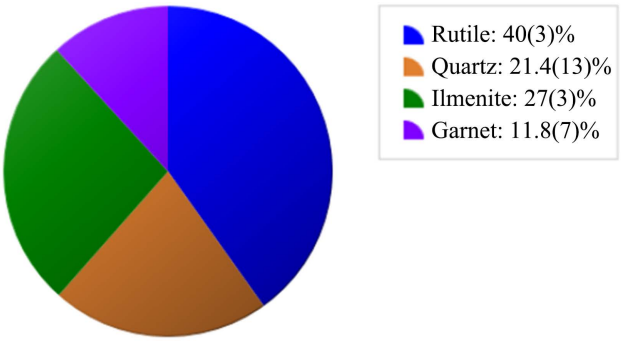

Figure 9. Pie chart showing the associated minerals in Rutile ores.

Table 8. Industrial/commercial applications of bauxite and Rutile ores associated minerals.

S/N	Associated Mineral	Industrial/Commercial Applications
1	Albite	Glass manufacture, as fillers, ceramics, paint and as extenders plastics
2	Garnet	Gemstones for jewelry and ornamentals and as abrasives
3	Illite	Illite as a major source of tradition ceramics is used in the production of cooking pots, plates, tiles and bricks.
4	Manufacture of a wide variety of electronics, fillers in Muscovite paint, plastics.	
5	Quartz	Essential raw material for the glass and foundry casting industries, water filtration, building of houses/roads and for support
6	Ilmenite	Used in paints, printing inks, fabrics, sunscreen, food and as cosmetics

attributed to crystallite size effects. The percentage of pure bauxite in the ore meets metallurgical grade (15 - 25)% and can be utilize in the commercial extraction for aluminium [18]. Similar mineralogy check was carried out for columbite ore in the mining locations of Yelwa-mbar Bokkos LGA, Plateau State, the main minerals found in the Columbite sample were Braunite, Cassiterite, Ilmenite, Quartz, and Zircon with each of these compounds having a phase information from the XRD pattern as were recorded for bauxite mineralogy [1].

5.2. Albite

Albite ($NaAlSi_3O_8$) as revealed in this research is one of the interlocking minerals of bauxite ore, it belongs to the plagioclase feldspar series. Albite is usually found together with quartz, mica, other feldspar minerals and sometimes iron oxides, ruffle, tourmaline, and hornblende. Albite minerals (soda-spar) together with microcline or orthoclase (potash-spar), and anorthite (calcium-spar) are the commercial feldspar minerals [19]. Its occurrence as an associated mineral from the X-ray diffraction of bauxite is consistent with its presence in the previous xrf of the mineral source from the same sample location.

The ore is used in glass manufacturing, in the production of ceramics, and in value-added applications such as fillers and extenders in plastics, paint, and rubber. They are, however, often associated with Fe and Ti impurities that decrease their economic value and hinder their application [20].

5.3. Garnet

In common natural occurrences, garnet is a silicate mineral belonging to the nesosilicate group, it is consist of isolated silicon tetrahedra [SiO_4^{4-}] bound together by other cations [21]. Its general formula is $X_3Y_2Si_3O_{12}$, where X is an eight fold coordinated site most commonly filled by a solid solution of divalent Fe, Mg, Ca, and Mn, and Y is a six fold-coordinated site typically filled by trivalent Al (*i.e.* the aluminosilicate garnets) or sometimes by Fe^{3+} or Cr. Garnet shows two distinctly different modes of occurrence; one is minute clusters distributed sporadically within the host skarn and the other is extremely narrow veinlets filling the hairline fractures or microcracks, which penetrate the host skarn. As an associated mineral of bauxite ore from the Wase exploration site, garnet presence is believably link to its occurrence in the soil as revealed in the xrf oxides (44.91%-SiO_2) result. It is typically used in gemstones for jewellery and ornamentals and as abrasives and fillers [22].

5.4. Illite

Illite occurs in various minerals ore such as in bauxite, rocks and clay, most times as illite/montmorillonite in argillaceous sediments having the same mineralogical properties and chemistry. Its occurrence as an associated mineral of bauxite in this research is consistent to its very high percentage recorded in the X-Ray Fluorescence result for bauxite ore and soil. Nowadays, the term "illite" refers to an aluminum-potassium mica-like, non-expanding, dioctahedral mineral, present in the clay fraction. Together with kaolinite, chlorite and smectite, illite is in fact one of the four major phases of clay-sedimentary rocks. Illite forms a series with an interlayer cation content from 0.6 to 0.85 with an approximate formula deduced from studies on natural materials: $K0.88Al_2(Si_3{\cdot}12Al0.88)O_{10}(OH)_2{\cdot}nH_2O$ [23]. There are many fields where illitic clays play an important role: illite is one of the major components of clays used in traditional ceramics for the production of cooking pots, plates, tiles and bricks. Of great importance is its application in the production of stoneware tiles, the top product in the market of traditional ceramics [24].

5.5. Muscovite

Muscovite ($KAl_2(Si_3Al)O_{10}(OH)_2$) also known as mica is the most common rock-forming minerals of pegmatite. As an associated mineral of bauxite ore, muscovite showed no link or fragmentation pattern with the X-ray fluorescence results for soil, sediment, plant roots and stem. Other micas occurring in pegmatites include but not limited to biotite, zinnwaldite, polylithionite and lepidolite.

The highly structural and chemical flexibility for micas make them become repositories for major, minor and trace elements that do not favorably enter into quartz and feldspars which are the major mineral phases [25]. Micas formed from higher evolved magma normally show enrichment in Li, Rb, Cs and F, with decrease in Mg, Ti and the K/Rb values, both from the external to internal zones in individual zoned bodies and from pegmatites with different degrees of evolution. Muscovite as the most common mica during the whole pegmatite evolution and among diverse pegmatites is a good petrogenetic indicator of pegmatite evolution and mineralization [26]. Muscovite can be cleaved into very thin transparent sheets that can substitute for glass, particularly for high temperature applications such as industrial furnace or oven windows. It is also used in the manufacture of a wide variety of electronics and as a filler in paints, plastics and wallboard [27].

5.6. XRD Peak Information of Rutile Ore

The X-ray diffraction result for rutile ore obtained from the Gwamlar, Kanam mineral location as observed in **Figure 8** revealed the interlocking minerals of rutile (40)%, quartz (21.4)%, ilmenite (27)% and garnet (11.8)% respectively. These minerals were found within the 2Θ range (27.5 to 35.6) and a peak value intensity of 31.1 to 100.0 cps as obtained from the diffractogram. The percentage of pure rutile from the ore meets metallurgical grade, showcasing this mineral location as a major source of rutile for industrial use. This analytical result is in unison with the XRD result obtained for tin and columbite ore crystals of the Yelwa-Mbar mining site, the diffraction of X-rays by the crystalline solid mineral sample results in a pattern of sharp bragg reflection characteristic of the different d-spacing of the ore. This is also similar with the result obtained for XRD analysis of bauxite ore as earlier reported.

5.7. Quartz

The mineralogy of rutile ore as another source of fine quartz revealed that there was about 21.4% of the mineral in the ore sample responsible for the presence of heavy metals in soil, sediment, plant roots and stem in the X-ray fluorescence samples. Quartz sand is the final product of rock weathering which is an important part of the rock cycle, it is an oxide of silicon with the chemical formula SiO_2, also known as silica [18]. In the plateau mineral industry, quartz is the major component of the abundant rock minerals in the state. The weathering of any quartz-bearing rock creates sand whether igneous, sedimentary, or metamorphic rocks. Quartz is used in a great variety of products and the term "quartz sand" in its finest form, as micro-silica it is used as an essential raw material for the glass and foundry casting industries, as well as in other industries such as ceramics, chemical manufacture and for water filtration purposes [1]. Before the advent of technology, quartz was used in baking. Other applications include construction of houses, roads and bridges and also used for support. The major

environmental issues associated with mineral-sand exploration is the contamination of water sources with chemicals used in mining operation such as chlorine, release of radiation hazards and food crop contamination with heavy metals [28].

5.8. Ilmenite

In the same vain, the XRD analysis of rutile ore revealed relatively 27% of ilmenite in the sample unveiling rutile as another source of the ore for industrial purpose. The high percentage of ilmenite recorded in the X-Ray diffraction of rutile ore is believed to be link to the presence of Fe and Ti oxides in the XRF results for soil and sediment samples. Ilmenite ($(Fe,Ti)_2O_3$) in itself is another important ore of titanium-oxide which is considered as weak magnetic mineral sand, grey-black in color and solid in form, industrially used in paints, printing inks, fabrics, sunscreen, food and as cosmetics [29]. The major environmental concern associated with the mineral-sands industry is the radiation hazards. Ionizing radiation is responsible for this radiation hazards. These are mostly associated with titanium-oxide mining operations. Other issues of concern are pollution of ground-water resources, mineral transport with heavy vehicles, dredging operations in fragile coastal area and clearing of forest [30].

6. Conclusions

Radionuclides ^{238}U, ^{232}Th, and ^{40}K were present in both soil samples received from the mineral vicinities around bauxite and rutile ore in various concentrations. These radionuclides released on the surface soil due to mining activities pose's a negative effect on the artisans and their surrounding water and soil. Estimating the representative limit index (RLI), activity utilization index (AUI), internal and external hazard indices (Hin and Hex) of these samples revealed values exceeding the radiation standards (>1) for soil. Lower concentrations were however obtained for Radium equivalent radioactivity (<370 Bq/Kg thereby keeping the external dose at (<1.5 mGy/h) and soil control samples.

The mineralogy analysis of bauxite ore in **Figure 5** unveiled the interlocking minerals of Bauxite (18)%, Albite (11)%, Garnet (15)%, Illite (6)% and Muscovite 2M1 (2)%. The X-ray diffractogram revealed that the ore and other minerals were obtained within the 2Θ range (9.18 to 64.4) and a peak value (intensity, cps) of 3400. Broadening of reflections due to instrumental factors were generally attributed to crystallite size effects. The pure bauxite percentage in the ore meets metallurgical grade (15 - 25)% and can be utilize in the commercial extraction of aluminum. These interlocking minerals of bauxite are of immense economic importance yet presenting issues of environmental concerns due to the presence of heavy metals such as Fe, Ti (albite), Fe, Cr (garnet), Al, K (illite) Li, Rb, Cs, Mg and Ti (muscovite). Similarly, the X-ray diffraction of rutile ore revealed the associated minerals of rutile (40)%, quartz (21.4)%, ilmenite (27)% and garnet (11.8). This percentage of pure rutile from the ore also meets metal-

lurgical grade, showcasing this mineral location as a major source of rutile for industrial use. The major environmental concern associated with the mineral-sands industry is the radiation hazards. These are mostly associated with titanium-oxide mining operations. Other issues of concern are pollution of ground-water sources from heavy metals, mineral transport with heavy equipments, dredging operations in fragile coastal area and clearing of forest.

Test of Significance

T-test at 95% confidence interval indicates that even though bauxite mineral vicinity soil had higher radio-hazards and metal concentration compared to rutile vicinity soil, the difference is not statistically significant. Bauxite Soil (Mean 41.52 SD 91.05), Rutile Soil (Mean 36.87 SD 80.69), $p > 0.05$.

Conflicts of Interest

The authors declare no conflicts of interest regarding the publication of this paper.

References

[1] Itodo, A.U, Wuana, R.A, Bulus, E.D and Davoe, D.B, (2019) Mineralogy and Pollution Status of Columbite-Tin Ore Contami-nated Soil. *Advanced Journal Chemistry-A*, **2**, 147-164.

[2] Odoh, C.K., Akpi, U.K. and Anyah, F. (2017) Environmental Impacts of Mineral Exploration in Nigeria and Their Phytoremediation Strategies for Sustainable Ecosystem. *Global Journal of Science Frontier Research*, **17**, 20-28.

[3] Bulus, E.D., Itodo, A.U., Wuana, R.A. and Eneji, I.S. (2023) Chemical Analysis of Bauxite and Rutile Ore, Contaminated Vicinity Soil, Sediment and Plants (Vigna Unguiculata) in Kanam and Wase, Plateau State-Nigeria. *Open Access Journal of Science Research*, **1**, 65-98.

[4] Lokeshwari, H. and Chandrappa, G.T. (2006) Impact of Heavy Metal Contamination of Belladur Lake on Soil and Cultivated Vegetation. *Current Science,* **91**, 622-627.

[5] Carla, M.R., Fulvia, C. and Subramanian, S. (2021) Remediation of Metal/Metalloid Polluted Soils. *Applied Science*, **11**, Article No. 4134. https://doi.org/10.3390/app11094134

[6] Kodom, K., Preko, K. and Boamah, D. (2012) X-ray Fluorescence (XRF) Analysis of Soil Heavy Metal Pollution from an Industrial Area. *Soil and Sediment Contamination,* **21**, 1006-1021. https://doi.org/10.1080/15320383.2012.712073

[7] Augustine, K.A., Adekunle, K.B. and Adeniyi, C.A. (2014) Determination of Naturalradioactivity and Hazard in Soil Samples in and around Gold Mining Area in Itagunmodi, South-Western, *Nigeria*, *Journal of Radiation Research and Applied Sciences*, **7**, 249-255. https://doi.org/10.1016/j.jrras.2014.06.001

[8] UNSCEAR (2000) Exposure from Natural Radiation Sources. United Nations Scientific Committee on the Effects of Atomic Radiation. Report to General Assembly. Annex B Exposure from Natural Radiation Sources. United Nations, New York. *Science World Journal*, **8**, 1-6.

[9] Jiya, S.N. and Musa, H.D. (2012) Impacts of Derived Tin Mining Activities on Lan-

duse/Landcover in Bukuru, Plateau State, Nigeria. *Journal of Sustainable Development*, **5**, 90-100. https://doi.org/10.5539/jsd.v5n5p90

[10] Abdulkarim, M.S., Umar, S., Mohammed, A. and Modelu, D. (2018) Determination of Radionuclides in Soil Samples Taken from Gura Topp (Jos) Using Sodium Iodide Thallium Detector Nai(Ti). *Nigerian Journal of Basic and Applied Science*, **26**, 30-34. https://doi.org/10.5455/NJBAS.291269

[11] Abdulkarim, M.S. and Umar, S. (2013) An Investigation of Natural Radioactivity around Gold Mining Sites in Birnin Gwari North Western Nigeria. *Research Journal of Physical Sciences*, **1**, 20-23.

[12] Jarus, P. (2023) A Brief Note on the Effects of Radiation on Environment. *Journal of Ecology and Toxicology*, **7**, Article ID: 1000153.

[13] Alam, M., Miah, N.M., Chowdhury, M.I., Kamal, M., Ghose, S. and Islam, M. (1999) Radiation Dose Estimation from the Radioactivity Analysis of Lime and Cement Used in Bangladesh. *Journal of Environmental Radioactivity*, **42**, 77-85. https://doi.org/10.1016/S0265-931X(98)00027-7

[14] El-Gamal, A., Nasr, S. and El-Taher, A. (2007) Study of the Spatial Distribution of Natural Radioactivity in Upper Egypt Nile River Sediments. *Radiation Measurements*, **42**, 457-465. https://doi.org/10.1016/j.radmeas.2007.02.054

[15] Al-trabulsy, H.A., Khater, A.E.M. and Habbani, F.I. (2011) Radioactivity Levels and Radiological Hazard Indices at the Saudi Coastline of the Gulf of Aqaba. *Radiation Physics and Chemistry*, **80**, 343-348. https://doi.org/10.1016/j.radphyschem.2010.09.002

[16] UNSCEAR (2000) Report to General Assembly with Scientific Annexes. "Sources and Effects of Ionizing Radiation", United Nations Sales Publications No. E.00.IX.3 Volume I: Sources and No. E.00.IX.4 (Volume II: Effects) United Nations, New York. *Nigerian Journal of Basic and Applied Science*, **26**, 30-34.

[17] Chandrasekaran, A., Ravisankar, R., Senthilkumar, G., Thillaivelavan, K., Dhinakaran, B. and Vijayagopal, P. (2014) Spatial Distribution and Lifetime Cancer Risk Due to Gamma Radioactivity in Yelagiri Hills, Tamilnadu, India. *Egyptian Journal of Basic and Applied Sciences*, **1**, 38-48. https://doi.org/10.1016/j.ejbas.2014.02.001

[18] Pekala, A. (2020) Silification of the Mesozoic Rocks Accompanying the Belchatow Lignite Deposite, Central Poland. *Geosciences*, **10**, Article No. 141. https://doi.org/10.3390/geosciences10040141

[19] Marinov, M., Valchev, A., Nishkov, I. and Grigorova, I. (2010) Feldspar Concentrates from Albite Granites**.** *Proceedings of* 2*nd International Symposium on the Processing of Industrial Minerals*, Vol. 2, 1-9.

[20] Vidyadhar, A., Hanumantha, R.K, Chernyshova, I.V, Pradip and Forssberg, K.S.E (2002) Mechanism of Amine-Quartz Interaction in the Absence and Presence of Alcohols Studied by Spectroscopic Methods. *Journal of Colloids and Interface Science*, **256**, Article ID: 127142. https://doi.org/10.1006/jcis.2001.7895

[21] Grew, E.S., Locock, A.J., Mills, S.J., Galuskina, I.O., Galuskin, E.V. and Hålenius, U. (2013) Nomenclature of the Garnet Supergroup. *American Mineralogist*, **98**, 785-810. https://doi.org/10.2138/am.2013.4201

[22] Caddick, M.J. and Kohn, M.J. (2013) Common Mineral, Uncommonly Useful. *Elements*, **9**, 427-432. https://doi.org/10.2113/gselements.9.6.427

[23] Rosenberg, P.E. (2002) The Nature, Formation, and Stability of End Member Illite. A Hypothesis. *American Mineral Journal*. **87**, 103-107. https://doi.org/10.2138/am-2002-0111

[24] Ferrari, S. and Gualtieri, A.F. (2006) The Use of Illitic Clays in the Production of

Stoneware Tile Ceramics. *Applied Clay Science*, **32**, 73-81. https://doi.org/10.1016/j.clay.2005.10.001

[25] Pichavant, M., Villaros, A., Deveaud, S., Scaillet, B. and Lahlafi, M. (2016) Influence of Redox State on Mica Crystallization in Leucogranitic and Pegmatitic Liquids. *The Canadian Mineralogist*, **54**, 559-581. https://doi.org/10.3749/canmin.1500079

[26] Li, J., Huang, X.L., He, P.L., Li, W.X., Yu, Y. and Chen, L.L. (2015) *In Situ* Analyses of Micas in the Yashan Granite, South China: Constraints on Magmatic and Hydrothermal Evolutions of W and Ta-Nb Bearing Granites. *Ore Geological Review*, **65**, 793-810. https://doi.org/10.1016/j.oregeorev.2014.09.028

[27] Zhou, Q., Qin, K., Tang, D. and Wang, C. (2022) A Combined EMPA and LA-ICP-MS Study of Muscovite from Pegmatites in the Chinese Altai, NW China: Implications for Tracing Rare-Element Mineralization Type and Ore-Forming Process. *Minerals*, **12**, Article No. 377. https://doi.org/10.3390/min12030377

[28] Shahjadi, H.F., Nazmul, H. and Parvez, M.A. (2016) Life-Cycle Environmental Impact Assessment of Mineral Industries. *Materials Science and Engineering*, **351**, Article ID: 012016.

[29] Law, E. and Lane, D.A. (2016) Pollution Caused by Waste from the Titanium Dioxide Industry. *Materials Science and Engineering*, **351**, 1-8.

[30] Haque, N., Hughes, A., Lim, S. and Vernon, C. (2014) Rare Earth Elements: Overview of Mining, Mineralogy, Uses, Sustainability and Environmental Impact. *Resources*, **3**, 614-635. https://doi.org/10.3390/resources3040614